

A RAPID PAPER-BASED COLORIMETRIC MOLECULAR TEST FOR SARS-COV-2 POINT-OF-CARE DIAGNOSTIC

by

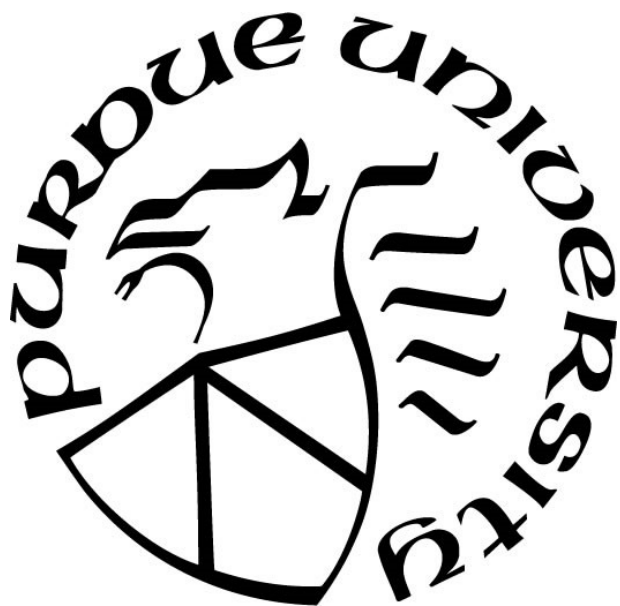
Jiangshan Wang

A Thesis

Submitted to the Faculty of Purdue University

In Partial Fulfillment of the Requirements for the degree of

Master of Science in Agricultural and Biological Engineering



School of Agricultural and Biological Engineering

West Lafayette, Indiana

May 2021

THE PURDUE UNIVERSITY GRADUATE SCHOOL
STATEMENT OF COMMITTEE APPROVAL

Dr. Mohit S. Verma, Chair

School of Agricultural and Biological Engineering

Dr. Rahim Rahimi

School of Materials Engineering

Dr. Caitlin Rose Proctor

School of Agricultural and Biological Engineering

Approved by:

Dr. Nathan S. Mosier

To my friends and family for their unconditional love and support.

ACKNOWLEDGMENTS

I am deeply grateful to my supervisor, Dr. Mohit S. Verma for his invaluable advice and continuous support during my master study. At many stages in my academic study, I benefited from his advice. His profound knowledge pushed me to sharpen my thoughts and brought my work to a higher level.

I wish to thank my committee members for their time, support, and the guidance throughout the preparation and review of this document.

My colleagues Josiah Levi Davidson provided data on primer designing. Ana Pascual-Garrigos and Andrés A Dextre provided the colorimetric dye screening experiment data. I would like to acknowledge them for their contribution to this thesis.

Thanks to Jordan Seville and Darby McChesney from PortaScience Inc. They helped with the final device designing and fabricated the device prototype.

To all the other members in the Verma Lab. Thank you for your kind help and support in all the time of my academic research and daily life.

TABLE OF CONTENTS

LIST OF TABLES	7
LIST OF FIGURES	8
LIST OF ABBREVIATIONS	10
ABSTRACT	11
1. INTRODUCTION	12
1.1 Background and Significance	12
1.2 Thesis Objectives	13
1.3 Organization of Thesis	13
2. LITERATURE REVIEW	14
2.1 SARS-CoV-2 and its international impact	14
2.2 Clinical Studies and Diagnostic Method for SARS-CoV-2	14
2.3 LAMP as an effective solution for diagnosing SARS-CoV-2	15
2.4 Current POC devices implementing LAMP	16
3. MATERIALS AND METHODS	17
3.1 Primer Design	17
3.2 Heat inactivated SARS-CoV-2 virus	17
3.3 Saliva Collection devices and fresh saliva collection	17
3.4 Fabrication and optimization of devices	18
3.4.1 Screening of paper-like materials	18
3.4.2 Device assembly	18
3.5 Optimization of composition of the assay	19
3.5.1 Screening of colorimetric dyes	19
3.5.2 Phenol red concentration determination	19
3.5.3 Replacing ammonium sulfate with betaine as LAMP destabilizing agent	20
3.5.4 Other LAMP assay formulation optimization	20
3.6 Determining LoD and Data Analysis	21
4. RESULTS AND DISCUSSION	23
4.1 Selection of saliva collection device	23
4.2 Optimization of the colorimetric assay	23

4.3	Design of paper-based devices.....	23
4.4	Validation with contrived samples.....	24
5.	CONCLUSIONS	44
	REFERENCES	45

LIST OF TABLES

Table 1: Bill of materials of a kit for Colorimetric LAMP device (sorted by % table contribution). Prices are based on academic laboratory prices from vendors.	25
Table 2: Assay characterization chart. Red highlights represent reactions greater than the threshold to consider a reaction as positive reaction. Green channel intensity is shown.	26

LIST OF FIGURES

Figure 1: LAMP detection on multiple papers: chromatography grade 1, anionic exchange nylon, cationic exchange nylon, polyether sulfone membrane, asymmetric sub-micron polysulfone (BTS 0.8), asymmetric sub-micron polysulfone (BTS 100) and hydroxylated nylon 1.2. b) Endpoint scans of the papers in panel a at 60 minutes and c) gel electrophoresis (2% agarose) scan of the extracted LAMP products at 60 minutes.	27
Figure 2: Schematic layout of the paper device.....	28
Figure 3: Typical colorimetric results of a negative and positive run. Controls are RT-LAMP reactions without LAMP primers included and positive reactions have 800 copies/ μ L spiked into 5% saliva.....	28
Figure 4: LAMP detection with increasing concentrations of calmagite (magnesium indicator). The lolB.3 primer set targeting <i>Histophilus somni</i> (HS) genomic DNA was used. Positive reactions were spiked with 5 μ L of HS gDNA at a concentration of 0.2 ng/ μ L. Negative reactions used 5 μ L of nuclease-free water. Total reaction volume is 25 μ L.	29
Figure 5: LAMP detection with increasing concentrations of Eriochrome® Black T (magnesium indicator). Primer sets and reaction conditions were the same as those in Figure S1.	30
Figure 6: RT-LAMP detection with increasing concentrations of cresol red sodium salt, Neutral red, Phenol red sodium salt, m-cresol purple, and m-cresol purple sodium salt in solution (pH indicator). The N.10 primer set targeting the N gene of SARS-CoV-2 was used. Positive reactions were spiked with 5 μ L of in-vitro transcribed N gene RNA at a concentration of 10.2 ng/ μ L. Negative reactions used μ L of nuclease-free water.	31
Figure 7: Endpoint gel electrophoresis scans of the RT-LAMP products (60 mins) in Figure 6.	32
Figure 8: LAMP detection with intercalating dye, Crystal violet a) in solution and b) associated in gel electrophoresis (2% agarose) scan of the products at 60 minutes.....	33
Figure 9: LAMP detection with increasing concentrations of Eriochrome® Black T on chromatography paper in PCR tubes (magnesium indicator).	34
Figure 10: LAMP detection with increasing concentrations of Phenol red on Grade 1 chromatography paper	35
Figure 11: Different LAMP formulations drying on Grade 1 chromatography paper.	36
Figure 12: Different LAMP formulations eliminating one component at a time and drying on Grade 1 chromatography paper. All LAMP formulations were adjusted to pH 8.0 according to a pH probe at 0 min. A color difference between conditions at 0 min is due to the fast acidification process once the reagent is applied to the paper.....	37
Figure 13: LAMP formulation using different betaine concentrations substituting ammonium ions as destabilizing agent. Reactions were performed in solution and Grade 222 chromatography paper simultaneously.	38

Figure 14: Colorimetric RT-LAMP results with the inclusion of Trehalose or Tween 20 at the given concentration. The orf7ab.I primer set was used and heat-inactivated SARS-CoV-2 at a concentration of 1×10^5 copies per reaction was spiked into 5% saliva.....	39
Figure 15: Colorimetric LoD on paper using Heat-inactivated virus at the indicated concentration in 5% saliva. The LoD of the assay was determined as 200 copies of virus per μL of whole saliva.	40
Figure 16: Box plot for the green channel intensity of 30 positive and 30 negative results of RT-LAMP on paper.....	41
Figure 17: Receiver-operator (ROC) curve for 30 positive and 30 negative results of RT-LAMP on paper.....	42
Figure 18: Color gradient of possible results derived from the colorimetric results of panel. ...	43

LIST OF ABBREVIATIONS

SARS-CoV-2:	Severe Acute Respiratory Syndrome Coronavirus 2
COVID-19:	Caused by infection with SARS-CoV-2
qPCR:	Quantitative Polymerase Chain Reaction
RT-PCR:	Real Time Polymerase Chain Reaction
RT-LAMP:	Reverse-Transcription Loop-Mediated Isothermal Amplification
LAMP:	Loop-mediated Isothermal Amplification
POC:	Point of Care
LFD:	Lateral flow Device
LoD:	Limit of Detection
CDC:	Centers for Disease Control and Prevention
JHU:	Johns Hopkins University
RNA:	Ribonucleic acid
dNTPs:	Deoxyribonucleotide Triphosphate
UDG:	Uracil DNA Glycosylase
UTP:	Uracil Triphosphate
ACE2:	Host cell receptor angiotensin-converting enzyme 2
TMPRSS2:	TM protease serine 2
ROC:	Receiver Operator Characteristic
IRB:	Institutional Review Boards

ABSTRACT

In the year of 2020, an international pandemic caused by severe acute respiratory syndrome coronavirus 2 (SARS-CoV-2) has afflicted tens of millions of people's life also disrupting global economics. Diagnostic testing is an important part of ensuring public health until a vaccine that has been shown to be safe and effective is made available to the general public. Most tests for detecting COVID-19 utilize quantitative polymerase chain reaction (qPCR) assays, which is a specific and relatively simple quantitative assay that could provide adequate sensitivity for diagnosing early infection. Although powerful, these lab-based molecular assays have a significant lag time, usually several days before receiving results. To satisfy the needs of different purposes (diagnostics, screening, and surveillance), a unified approach is impractical. This thesis presents an alternative testing method supporting the current procedure of point of care (POC) testing and in community testing. This paper-based test overcomes the limitations of current testing methods by utilizing reverse-transcription loop-mediated isothermal amplification (RT-LAMP) and receiving the result on-site by a color change in the presence of the virus within 60 minutes. The test utilizes untreated freshly collected saliva, a less invasive specimen, as the sample and possesses a limit of detection (LoD) of 200 copies of virus per microliter of whole saliva with an analytical sensitivity of 97% and analytical specificity of 100%. The test requires minimal operator training and could be fabricated on a large-scale using roll-to-roll methods. Since the test is based on nucleic acids, the testing platform itself lends to further applications including food safety monitoring, animal diagnostic, etc. simply by changing the specific primers.

1. INTRODUCTION

1.1 Background and Significance

Since the first identified case of COVID-19 in Wuhan, China, in December 2019, it has caused more than 42,000 deaths in the United States (CDC, January 2021) and 2,122,872 global death (JHU, January 2021). As a highly contagious virus that is transmitted mostly through respiratory droplets (Mohapatra et al., 2020), testing of people who is at high risk of exposure and who show symptoms of infection, such as trouble breathing or loss of sense of smell and taste, would reduce the chances that they would infect others and allowing them to seek medications early. Identifying symptomatic and asymptomatic individuals in a timely manner would be critical to halting the pandemic.

The most extensively used COVID-19 diagnostic tests are RT-PCR molecular tests. The advantage of this test is that the amplification and analysis are done simultaneously in a closed system which would minimize the false-positive results caused by amplification product contamination (Tang et al., 2020). At a local medical facility, an individual would receive a nasal (nasopharyngeal) swab by a trained professional. The swabs would be sent to central laboratories where machines process them in the sequence of genetic extraction, genetic amplification, and sample analysis. Best in class RT-PCR assay could demonstrate a limit of detection of ~100 copies of viral RNA per milliliter of transport media. Although very powerful, these lab-based molecular assays have a significant lag time, usually several days before receiving results. The test could only guarantee the individual was negative/positive at the time of sampling thus relatively poor in timeliness.

Here, I show a detection assay that can detect the virus in saliva within 60 minutes utilizing a colorimetric response which can be read using naked eye. This assay requires minimal operator training and instrument (an external heater). This format of tests is amenable to a roll-to-roll fabrication and is anticipated to cost ~\$10/test (Table 1). The LoD of this assay is 200 copies / μ L saliva. The sensitivity (positive predictive value) is 96.7 % and the specificity (negative predictive value) is 97.8 %. Due to the simplicity and scalability of this test, I envision that it will be used widely. Since the test is a molecular test, it can be rapidly adapted for future applications including food safety monitoring, animal diagnostic, etc. simply by designing and screening new primer sets.

1.2 Thesis Objectives

The objective of this work is to:

1. Design and characterize a liquid-based colorimetric RT-LAMP assay that can be used to detect SARS-CoV-2 in human saliva samples.
2. Optimize the self-developed colorimetric assay to satisfy the condition of working on a paper-based format.
3. Develop the assay into a POC device and propose a novel testing platform for future molecular detections.

1.3 Organization of Thesis

This thesis is organized in a traditional style format.

2. LITERATURE REVIEW

2.1 SARS-CoV-2 and its international impact

Severe acute respiratory syndrome coronavirus 2 (SARS-CoV-2) is a highly contagious pathogenic virus first identified as the cause of a cluster of pneumonia cases in Wuhan, China. Since first identified, it has caused more than 42,000 deaths in the United States (CDC, January 2021) and 2,122,872 global death (JHU, January 2021). Meanwhile, the coronavirus pandemic has had a significant effect on the global economy, with estimates of a -2.8 percent fall in global GDP in 2020, and more than 15% in some nations (Fernandes, 2020).

SARS-CoV-2 is a single-stranded RNA virus that causes respiratory infection and presents symptoms such as fever, cough, shortness of breath, etc. It is one of the seven known coronaviruses to infect humans (229E, NL63, OC43, HKU1, SARS-CoV, MERS-CoV, and SARS-CoV-2). 229E, NL63, OC43, and HKU1 only result in mild symptoms while SARS-CoV, MERS-CoV, and SARS-CoV-2 could cause severe symptoms with fatality rates of 10%, 37%, and 5%, respectively (Huang et al., 2020). Infected individuals, whether symptomatic or asymptomatic, can be contagious and spread the virus to others. The majority of transmissions, according to current evidence, occur when an infected person is in near or direct contact with another person.

The entire viral genome of SARS-CoV-2 was characterized by metagenomic next-generation sequencing which is 29,881 nt in length (GenBank MN988668) (Chen et al., 2020). The RdRp (RNA-dependent RNA polymerase), E (envelope), N (nucleocapsid), and S (spike glycoprotein) genes are the targets most frequently used in SARS-CoV-2 molecular testing assays.

The virus entry into host cells is mediated by its spike glycoprotein (S-glycoprotein). When the S-glycoprotein proteins covering the surface of SARS-CoV-2 bind to the host cell receptor angiotensin-converting enzyme 2 (ACE2), TM protease serine 2 (TMPRSS2) activates S-glycoprotein facilitating the virus entry (Huang et al., 2020). The virus goes through a process of replication, assembly, and virions release once it enters the cell.

2.2 Clinical Studies and Diagnostic Method for SARS-CoV-2

At the early stage of this pandemic, chest CT was suggested for diagnosing SARS-CoV-2 due to its reliability and high sensitivity 97% (95% confidence interval: 95%, 98%; 580 of 601

patients) while molecular tests, RT-PCR for throat swab samples, were reported to be approximately 30%–60% accurate (Ai et al., 2020). The current gold standard is to perform a RT-PCR on nasopharyngeal specimens. The state-of-art assay demonstrates a LoD of approximately 100 copies of viral RNA per milliliter of transport media, corresponding to a clinical sensitivity of 90%, or 9 in 10 infected individuals (Arnaout et al., 2020) while most other RT-PCR assay demonstrates a clinical sensitivity of 54 - 77% (Kucirka et al., 2020). This is because virus loads could span multiple order of magnitudes in nasopharyngeal swabs from 9 copies/mL to 2.5×10^9 copies/mL (n=6037) and from about 10^4 copies/mL to 10^8 copies/mL in saliva samples (n=397) (Arnaout et al., 2020; Zhu et al., 2020).

For molecular tests, specimens could be collected in various ways, most commonly nasopharyngeal swabs, oropharyngeal swabs, and saliva collection. Both nasopharyngeal swabs and oropharyngeal swabs collections require trained specialists. Only saliva specimens are appropriate for self-collection. The specimens would be placed immediately in a sterile transport tube containing transportation media and would be sent to central laboratories for molecular testing. Results could be expected the same day or 1-3 days depending on the testing location.

2.3 LAMP as an effective solution for diagnosing SARS-CoV-2

Loop mediated isothermal amplification (LAMP) offers a unique approach to detecting pathogens in clinical samples. It is a rapid, low-cost, highly selective isothermal amplification that employs a DNA polymerase and a set of six specially designed primers. Bst DNA Polymerase, a portion of the *Bacillus stearothermophilus* DNA Polymerase protein, has an inherent strand displacement activity between 60 °C-65 °C, only a single temperature is required for the reaction to be conducted. The reaction could be carried out on a cheap, simple heat source, such as an incubator or a water bath, overcoming the limitation of traditional PCR methods which demand expensive thermocyclers. Due to the simplicity and scalability, LAMP is more satisfactory for in field situations or in communities as a preliminary screening test.

In addition, Bst DNA polymerase is more robust compared to PCR DNA polymerase. PCR inhibitors are commonly found in untreated biological fluids such as blood, stool, and urine, which can lead to false negative results (Schrader et al., 2012). As a result, expensive and time-consuming DNA or RNA extraction and purification steps are needed to obtain a sensitive result from a PCR

assay (Kaneko et al., 2007). The robustness of the LAMP Bst polymerase to PCR inhibitors makes it capable of performing a rapid and sensitive pathogen detection of unpurified clinical samples (Francois et al., 2011; Lalli et al., 2020).

2.4 Current POC devices implementing LAMP

Long-term dry storage of LAMP reagents serves the purpose of prolonging the product's shelf life. It is reported that all necessary LAMP reagents, including WarmStart Bst 2.0 polymerase, retained a high level of activity after dry storage in a glass fiber matrix with preservatives (10% trehalose, 2.5% dextran) up to one year at 22 °C (Kumar et al., 2020).

To have a ready-to-use assay, researchers tried drying the complete LAMP mixture onto the inner side of PCR tube caps (Hayashida et al., 2015). The template is added inside the tube followed by turning the tube upside down, using the template to reconstitute the dried LAMP reagents. There are also studies attempting to incorporate LAMP onto a paper-based device, such as a multi-layer real-time fluorescence LAMP for detecting bacterial meningitis (Seok et al., 2017). A sample flow splitting design enables the device to simultaneously detect three different meningitis DNA samples in a single device. Another approach of incorporating LAMP onto a paper-based device is combining it with a lateral flow device (LFD) (Mallepaddi et al., 2018). After the LAMP assay is performed, the samples were loaded on the well of a lateral flow dipstick. Amplified samples exhibited two colored lines, whereas the unamplified samples exhibited the control line only. However, most of these devices require DNA extraction, which really defeats the idea of POC testing.

3. MATERIALS AND METHODS

3.1 Primer Design

The LAMP primer set used in this thesis was designed by my colleague Josiah Levi Davidson.

Primer	Sequence (5' - 3')
Orf7ab.I F3	ACTTAAAAACACAGTCTGTACC
Orf7ab.I B3	TCAAAAGCCCTGTATACGA
Orf7ab.I FIP	TGACTGAAGCATGGGTTCGCGTCTGCGGTATGTGGAAAG
Orf7ab.I BIP	GCTGATGCACAATCGTTTTTAAACGCATCAGTACTAGTGCCTGT
Orf7ab.I LF	GAGTTGATCACAACTACAGCCATA
Orf7ab.I LB	TTGCGGTGTAAGTGCAGCC

All oligonucleotides were purchased from Life Technologies and used desalting for purification.

3.2 Heat inactivated SARS-CoV-2 virus

Heat-inactivated SARS-CoV-2 was purchased from ATCC (ATCC VR-1986HK). This product is a preparation of Severe acute respiratory syndrome-related coronavirus 2 (SARS-CoV-2) strain 2019-nCoV/USA-WA1/2020 that has been inactivated by heating to 65 °C for 30 minutes and is therefore unable to replicate (reproduced from product description for ATCC VR-1986HK).

3.3 Saliva Collection devices and fresh saliva collection

Three commercial saliva collection devices were selected to evaluate their effect on the RT-LAMP reaction in saliva. They were primarily selected based on their respective mechanisms when collecting saliva. The three devices were “Saliva Sampler™” produced by StatSure Diagnostic Systems, Inc., “Pure•SAL™” produced by Oasis Diagnostics®, and “Super•SAL™” also produced by Oasis Diagnostics®. The StatSure Saliva Sampler™ provides a tube containing a buffer (Buffer 2000) used to collect saliva from a patient. Super•SAL uses a cylindrical absorbent pad and a collection tube to standardize the collection of saliva by removing any solid contaminants and mucinous material. Pure•SAL operates on a similar mechanism but includes an

additional filter in the collection tube to remove contaminants and is supposed to be optimized for RNA retrieval. Pure•SAL was chosen for this study.

Fresh saliva was collected from participants who enrolled in the study in accordance with Purdue University IRB Protocol # IRB-2020-527. Participants who reported receiving a positive diagnosis for COVID-19 within the past 60 days were not permitted to donate. Saliva was collected from participants only after they were made aware of the study's protocols and procedures and gave informed consent. Samples were assigned an ID based on the donor, date of sample collection, and method used for collection. No identifying information on participants was recorded.

3.4 Fabrication and optimization of devices

3.4.1 Screening of paper-like materials

Paper-like materials were selected based on four primary criteria: stability of formulation when dried on the substrate, intensity of color change when rehydrated with the sample, ability of the sample to evenly wick throughout the paper-based substrate, ability to remain inert throughout the reaction, and ability to demonstrate a color change upon amplification (Figure 1). Whatman Grade 1 chromatography paper was originally tested and used for optimization. When assembling two strips together, it was observed that the distribution of fluid was uneven because of the large area of the Grade 1 chromatography paper needed. Thus, with the help of PortaScience Inc., we selected Ahlstrom Grade 222 chromatography paper, which thickness is 0.83mm, thicker than Grade 1 chromatography paper 0.18 mm. Grade 222 allowed the paper strips to be 5 mm x 6 mm in size while adding the same amount of sample and showing a better color contrast after amplification.

3.4.2 Device assembly

The final device has dimensions of 5 mm x 6 mm (reaction pads dimension), 24 x 54 mm (testing strip dimension) and consisted of: Melinex 454 (3 mil thickness) backing, double-sided adhesive (ArClean 90178), 2 reaction pads (Ahlstrom Grade 222 Paper), and polystyrene spacers (Figure 2). The sample volume loaded onto the device was determined by incrementally increasing the volume until the reaction strips were saturated. This volume was then used as the final sample volume added and was determined to be 25 μ L per reaction pad.

3.5 Optimization of composition of the assay

3.5.1 Screening of colorimetric dyes

Several classes of colorimetric indicators were screened including magnesium indicators, pH indicators, and DNA intercalating indicators. Screening criteria included color contrast between positive and negative results, the concentration of indicator, time to visually observable result, and stability of indicator for long-term storage. For magnesium indicators, we screened Calmagite (CAS# 3147-14-6) (Figure 4) and Eriochrome® Black T (EBT, CAS# 1787-61-7) (Figure 5). For pH indicators, we screened Bromothymol Blue (CAS# 76-59-5), Acid Fuchsin (CAS# 3244-88-0), Cresol red (CAS# 1733-2-6), Cresol red sodium salt (CAS# 62625-29-0), Phenol red (CAS# 143-74-8), Phenol red sodium salt (CAS# 34487-61-1), m-Cresol purple (CAS# 2303-01-7), m-Cresol purple sodium salt (CAS# 62625-31-4), and Neutral red (CAS# 553-24-2) (Figure 6). The only DNA intercalating dye that we screened was Crystal violet (CAS# 548-62-9) (Figure 8).

As shown in Figure 9, the magnesium indicators were not able to produce a consistent color change on paper. Additionally, we faced difficulty being able to stabilize the Crystal violet in solution to be a feasible indicator for the RT-LAMP reaction. As a result, we focused on pH indicators and selected indicators that had a color change around pH 6.5. After screening these pH indicators, we selected the indicator with the most consistent and the most dynamic color change. As a result, we elected to use Phenol red as our indicator.

3.5.2 Phenol red concentration determination

To provide more obvious color differences between negative results and positive results, also not inhibiting the reaction itself, phenol red concentration optimization was done on Grade 1 chromatography paper. Figure 10 shows that both 250 μ M and 500 μ M of phenol red per reaction display optimal results. Lower dye concentration requires fewer protons generated for a color change, whereas longer incubation time is needed for higher concentration phenol red paper pads to differentiate positives from negatives. Thus, phenol red concentration was settled on 250 μ M per reaction.

3.5.3 Replacing ammonium sulfate with betaine as LAMP destabilizing agent

After applying LAMP reagents to paper and leaving it to dry, the reaction pad turns yellow even without adding templates. The color change happens fast within 10 minutes. After complete drying, the paper was not able to restore red color by rehydrating with the template. The paper would turn red if an alkaline solution is added indicating the LAMP reaction mix is acidifying while leaving in an ambient environment due to an unknown reason. A concentrated strong buffer, Tris-HCl, was added to the homemade LAMP reaction mix to prevent the paper's acidification, however, the addition of buffer did not resolve the issue (Figure 11).

A leave-one-out approach was used to understand which component in the LAMP assay formulation is causing this yellowing issue. Ammonium sulfate, potassium chloride, magnesium sulfate, dNTPs, Tween 20, Bst 2.0 WarmStart® DNA Polymerase, and WarmStart® RTx Reverse Transcriptase were excluded from the mix one-by-one. A commercial colorimetric LAMP mix (WarmStart® Colorimetric LAMP 2X Master Mix) was also used as a control in this experiment. Figure 12 shows that aside from the paper strips excluding ammonium sulfate, all paper strips turned yellow within 10 minutes. Since sulfate ion is present from magnesium sulfate, it was determined that it is the ammonium ion that is contributing to paper acidification.

The ammonium ion has a destabilizing effect in a DNA amplification process, especially on weak hydrogen bonds between mismatched primer-template base-pairing, thereby enhancing amplification specificity. Potassium ion, similar to the stabilizing function of magnesium ion, promotes primer annealing and duplex formation during the polymerization process, while ammonium ion destabilizes duplex formation by interacting with hydrogen bonds between the bases (*PCR Setup—Six Critical Components to Consider - US*, n.d.).

A series of destabilizing agents that function similarly to ammonium ion were screened with the help of PortaScience Inc. and was decided to substitute it with betaine. Figure 13 shows that it was able to perform LAMP with three different concentrations of betaine both in solution LAMP and paper LAMP. Betaine concentration was set to 20 mM.

3.5.4 Other LAMP assay formulation optimization

RT-LAMP reaction components including potassium chloride, magnesium sulfate, Warmstart RTx Reverse Transcriptase, Warmstart Bst 2.0 Polymerase, dNTPs, betaine, Tween 20,

Antarctic UDG were first set at concentrations as indicated by the product literature for NEB colorimetric LAMP assay (Nathan et al., 2018). These components were then optimized by titrating each component from 0.25X liquid concentration to 5X or higher for paper LAMP assay. The optimal concentration was determined by the speed of the LAMP reaction, the contrast between positive and negative LAMP results at 60 minutes reaction time, and the reduced amount of non-specific amplification.

Buffers were excluded since the inclusion of these buffers required more time to observe a color change. Furthermore, processing the saliva with the Pure·SAL saliva collection device standardized the sample pH, rendering buffers unnecessary.

Assay stabilizing and resuspending additives such as trehalose, BSA, and Tween 20 were also added to increase the shelf-life of the paper assay after complete drying. To optimize the concentration of each component added, trehalose was titrated from 0 to 15% w/v using increments of 5%, BSA was titrated from 0 to 1.25 mg/mL using increments of 0.2 mg/mL, and Tween 20 was titrated from 0 to 2% v/v using increments of 0.5%. The optimal concentrations for trehalose, BSA, and Tween 20 were 10% w/v, 0.626 mg/mL, and 1% v/v, respectively.

UDG and dUTPs were included to reduce carryover contamination, which is common in LAMP workflows. Concentrations of UDG and dUTPs were determined based on values reported in prior literature (Hsieh et al., 2014).

3.6 Determining LoD and Data Analysis

Multiple serial dilutions of heat-inactivated virus in fresh saliva were made (Fresh saliva was first diluted to 5% v/v. Heat-inactivated virus was spiked into 5% saliva creating a serial dilution of 2.5 copies/ μ L– 400 copies/ μ L. These dilutions represent 50 copies/ μ L – 8000 copies/ μ L virus concentration in undiluted whole saliva samples) and were used as templates on paper devices to establish a baseline LoD. Reactions were run in triplicate on 5 mm x 6 mm reaction pads (Ahlstrom Grade 222 Paper) for each viral concentration and heated to 65 °C in a standard 75 L biological incubator (Fisherbrand Isotemp Microbiological Indicator, 15-103-0513) for 60 minutes. The color of the reaction pads at different time points was recorded by scanning the pads on a tabletop scanner (Epson Perfection V800 Photo Color). The LoD for a primer set was determined by the lowest viral concentration that resulted in a strong color change in all three replicates.

After determining an LoD of 200 copies/ μ L in saliva (Figure 15), the sensitivity and specificity were determined using 30 contrived positive samples of 200 copies/ μ L (1x LoD – 10 samples), 400 copies/ μ L (2x LoD – 10 samples), 800 copies/ μ L (4 samples), 8000 copies/ μ L (3 samples), 80,000 copies/ μ L (3 samples) and 30 NTC negative saliva samples.

The color of the reaction pads at different time points was recorded by scanning the pads on a tabletop scanner (Epson Perfection V800 Photo Color). For the sensitivity and specificity study, each pad was individually selected and analyzed with ImageJ for RGB color intensity. Green color intensities for all pads were extracted and were arranged in a table ordered by virus concentrations (Table 2). Table values were then converted to a box plot (Figure 16) formatted by OriginLab® OriginPro, to display amplification differences between positive and negative tests visually.

A receiver operator characteristic (ROC) curve (Figure 17) was generated by comparing all reaction pads' green color intensity data and cross-reactivity to a predefined threshold via binary classifications to assess positive vs. negative reactions. Various thresholds at an increment of 1 Green value were tested and used to calculate the true positive rate and false positive rate for each threshold classification. Diagnostic sensitivity and specificity of the LAMP assay were defined as the true positive rate and 1-false positive rate for the lowest threshold value that created the most significant difference in sensitivity between the ROC curve and the random chance line. Accuracy was determined by taking the area under the ROC curve. The sensitivity was calculated as a ratio of the number of true positives to total positives, including false-positive amplification. The specificity was calculated as a ratio of true negatives to total negatives, including false negatives.

4. RESULTS AND DISCUSSION

4.1 Selection of saliva collection device

A sponge-based collection device (Oasis Diagnostics® Pure·SAL) was selected to eliminate food particles from collected saliva. This device is commercially available and easy to use. In preliminary studies, the differences in performance of three saliva collection devices were evaluated, Pure·SAL provided the least variance in the day-to-day performance of the assay. In addition, Pure·SAL can eliminate host-to-host saliva pH differences by setting the treated saliva to a consistent pH of 8.0.

4.2 Optimization of the colorimetric assay

Although LAMP assay usually reports amplification by a fluorescent reporter, they would require an additional ultraviolet (UV) light source to be read by the naked eye; thus, we developed a colorimetric assay using phenol red as an indicator. Polymerization of DNA produces protons and phenol red is responsive to pH. The challenge lies in overcoming the buffering capacity of saliva to measure changes in pH. We determined that obtaining a significant color change in a timely manner was only possible by using diluted saliva (5% final concentration) since at this concentration, the buffering capacity, as well as the concentration of interferents (e.g., RNase), are reduced. It is reported that in a liquid LAMP assay, incorporating guanidine hydrochloride could help with improving the LoD and sensitivity (Zhang et al., 2020). However, guanidine hydrochloride could not be incorporated in the paper-based assay because it caused a significant color change when the reagents were dried.

4.3 Design of paper-based devices

Paper is widely used in pH indicators and urine strips and thus has the potential to be scaled up to millions of devices (Yetisen et al., 2013). Cellulose is commonly used for these applications, but we noticed that when the RT-LAMP reagents are placed on paper, they change color over time even when no template is present, and no amplification is taking place. This color change could be due to acidification of the reagents (due to degassing of ammonia from the RT-LAMP mixture). We could isolate this issue to ammonium sulfate but could not conclusively determine the cause

of this color change (Figure 12). We overcame this challenge by replacing the ammonium sulfate with betaine (Figure 13). In addition, we determined that the addition of trehalose and Tween 20 helped the reaction performance on paper and thus, included these in our formulation (Figure 14).

In order to conduct the assay in a sealed container, we chose a simple “1 x 1” re-sealable plastic bags. After loading the sample on the paper-based device, the device goes is placed in the bag and is placed then in an incubator (at 65 °C for 60 minutes). The bag was then removed and read visually (Figure 3) against a color chart (Figure 18).

4.4 Validation with contrived samples

After determining an LoD of 200 copies/ μ L in saliva (Figure 15), we created contrived samples of 200 copies/ μ L (1x LoD – 10 samples), 400 copies/ μ L (2x LoD – 10 samples), 800 copies/ μ L (4 samples), 8000 copies/ μ L (3 samples), 80,000 copies/ μ L (3 samples). We used aliquots of pooled freshly collected saliva (30 aliquots) as our negative samples. and quantified the results using image processing (Table 2). A ROC curve was generated to choose the most appropriate cut-off for the assay. The assay specificity is 100 % and the sensitivity is 97%.

4.5 The balance between time and sensitivity

While developing the colorimetric assay, there was an ever-present balance between assay response time and assay sensitivity. Saliva, an extracellular fluid produced in salivary glands, comprises 99.5% water and many other important substances. Saliva has a normal pH range of 6.2-7.6 with 6.7 being the average pH (Baliga et al., 2013). There are three possible buffer systems in saliva, i) phosphate buffer, ii) carbonic acid/bicarbonate buffer, iii) protein buffer. Due to the inherent feature of a pH-dependent test, the response time is highly dependent on these external buffering systems. With whole saliva samples, the protons generated by the LAMP reaction were not enough to break the buffering capacity of saliva. The most operable and user-friendly pretreatment would be diluting the saliva concentration, which simultaneously would be diluting the buffer systems to minimize the effect of the external buffer. The dilution will also impair the sensitivity of the assay. In order to meet the criteria of receiving a test result within 60 minutes, we settled diluting the whole saliva to 5% v/v.

Table 1: Bill of materials of a kit for Colorimetric LAMP device (sorted by % table contribution). Prices are based on academic laboratory prices from vendors.

Item	Supplier	Catalog #	Quantity	Units	Price (USD)	Unit price	Scrap rate	Corrected Unit Price	# of units /device	Contribution to cost /device	% Contribution to total cost
Device											
Warmstart RTx Reverse Transcriptase	New England Biolabs	M0380 L	0.125	mL	266	2128.0000	0.1000	2340.8000	0.0020	4.6816	31%
dNTPs (100 mM)	Invitrogen	10-297-018	0.25	mL	320	1280.0000	0.1000	1408.0000	0.0028	3.9424	26%
Warmstart Bst 2.0 Polymerase	New England Biolabs	M0538 M	0.06667	mL	312	4680.0000	0.1000	5148.0000	0.0003	1.3728	9%
Melinex 454 (3 mil thickness)	Tekra	454	59	sheets	101.48	100.0000	0.1000	110.0000	0.0004	0.0426	0%
orf7ab.1 Primer Mix	Life Technologies	N/A	12500	reactions	357.28	0.0286	0.1000	0.0314	1.0000	0.0314	0%
Double White Opaque Polystyrene Litho Grade 20 mil	Tekra	842676	25	sheets	4	100.0000	0.1000	110.0000	0.0001	0.0082	0%
Saaticare Hyphyl	SAATI	PES 105/52	1	sheets	100	100.0000	0.1000	110.0000	0.0001	0.0069	0%
Ahlstrom Grade 222 Paper	Ahlstrom - Munksjo	22281416	100	sheets	62.82	0.6282	0.1000	0.6910	0.0027	0.0019	0%
8.5" x 350 ft. Flexmount double sided tape	Flexcon	DF051521	7	roll	544.32	77.7600	0.1000	85.5360	0.0000	0.0012	0%
Betaine	Millipore Sigma	B0300-5VL	585.75	g	89.8	0.1533	0.1000	0.1686	0.0002	0.0000	0%
Tween 20	Sigma Aldrich	P9416	100	mL	27.9	0.2790	0.1000	0.3069	0.0003	0.0001	0%
Phenol Red Sodium Salt	Sigma Aldrich	114537	25	g	90.2	3.6080	0.1000	3.9688	0.0094	0.0373	0%
Potassium Chloride	Sigma Aldrich	P9541	500	g	43.4	0.0868	0.1000	0.0955	0.0007	0.0001	0%
Magnesium Sulfate	Sigma Aldrich	M2773	500	g	54.69	0.1094	0.1000	0.1203	0.0004	0.0000	0%
Antarctic UDG	Fisher Scientific	50-591-114	100	uL	69.3	0.6930	0.1000	0.7623	0.0050	0.0038	0%
dUTP	Fisher Scientific	FERRO133	250	uL	59.14	0.2366	0.1000	0.2602	0.0875	0.0228	0%
Sub-Total:										10.25	67%
Cartridge											
2 x 2" 2 Mil Reclosable Bags	ULINE	S-1690	1000	bags	18	0.0180	0.1000	0.0198	1.0000	0.0198	0%
Sample Collection											
Super SAL Universal Saliva Collection System	Oasis Diagnostics	SSAL-601	100	devices	460	4.6000	0.1000	5.0600	1.0000	5.0600	33%
Total:										15.33	

Table 2: Assay characterization chart. Red highlights represent reactions greater than the threshold to consider a reaction as a positive reaction. Green channel intensity is shown.

Virus Concentration (copies/ μ L)	Negative		Virus Concentration (copies/ μ L)	Positive	
	Control	Reaction		Control	Reaction
N	62.143	72.385	200	90.799	155.474
N	69.964	82.552	200	103.324	134.056
N	75.288	54.787	200	57.15	128.006
N	91.669	81.586	200	101.325	159.949
N	66.397	111.311	200	103.455	140.54
N	51.218	65.227	200	96.82	143.288
N	93.484	120.675	200	86.761	151.166
N	129.392	112.561	200	80.676	111.159
N	35.949	78.955	200	75.139	138.605
N	88.288	73.393	200	99.727	124.097
N	43.75	58.557	400	45.036	143.297
N	46.984	76.041	400	106.895	152.34
N	56.189	73.824	400	83.955	155.86
N	108.311	82.237	400	108.1	145.705
N	78.537	114.994	400	97.018	156.268
N	74.093	77.479	400	113.906	149.828
N	75.737	83.126	400	69.511	152.558
N	57.246	65.671	400	82.225	151.84
N	37.945	45.382	400	111.301	148.551
N	65.023	57.845	400	106.933	162.822
N	73.824	82.16	800	39.899	164.127
N	85.683	79.598	800	99.348	128.157
N	83.095	69.636	800	97.673	122.956
N	58.178	76.3	800	56.071	181.314
N	72.475	85.94	8000	43.304	198.597
N	57.101	84.81	8000	91.269	183.618
N	64.097	56.475	8000	110.869	170.227
N	75.657	115.178	80000	76.983	178.015
N	26.828	77.019	80000	86.421	174.821
N	64.355	74.335	80000	80.199	174.745

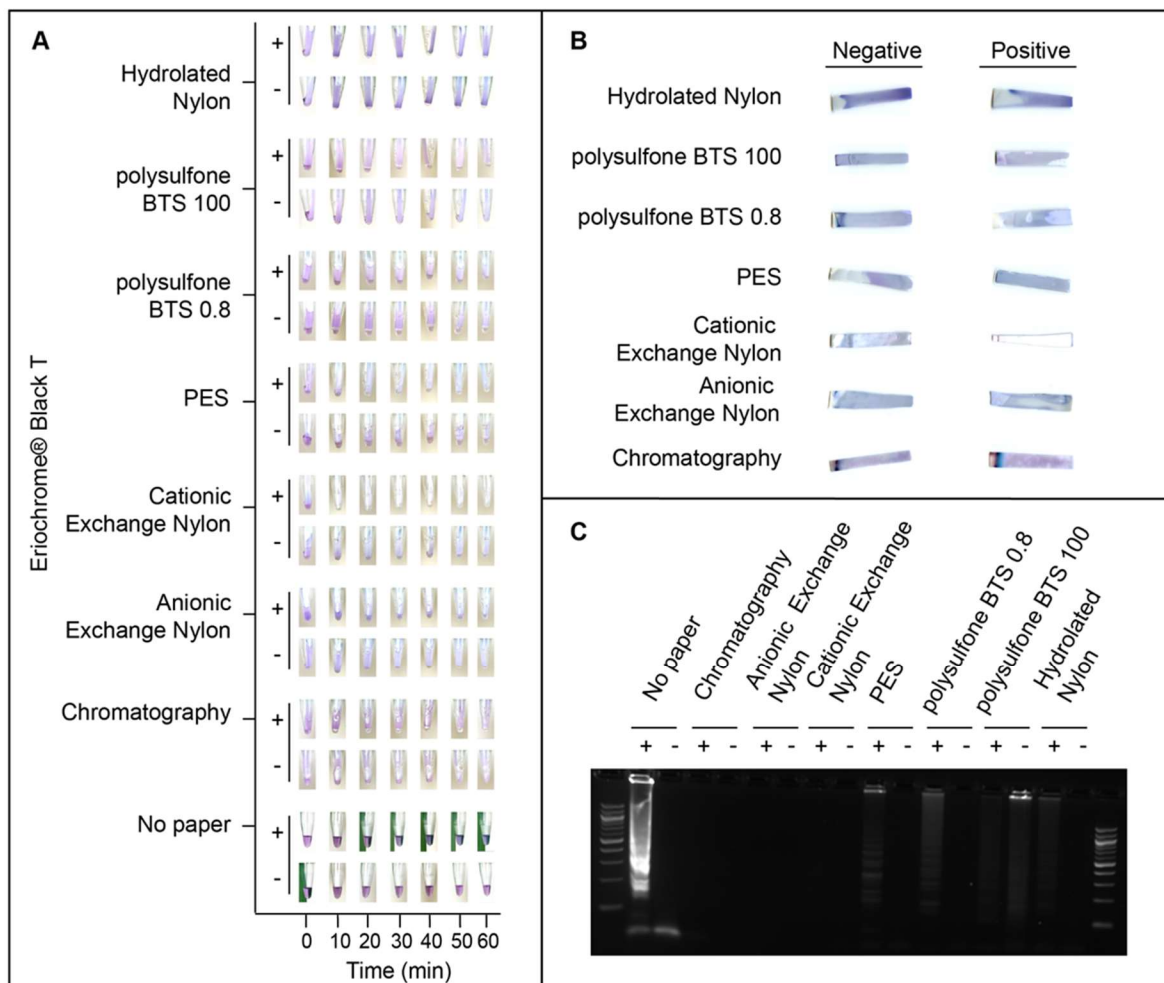


Figure 1: LAMP detection on multiple papers: chromatography grade 1, anionic exchange nylon, cationic exchange nylon, polyethersulfone membrane, asymmetric sub-micron polysulfone (BTS 0.8), asymmetric sub-micron polysulfone (BTS 100), and hydroxylated nylon 1.2. b) Endpoint scans of the papers in panel a at 60 minutes and c) gel

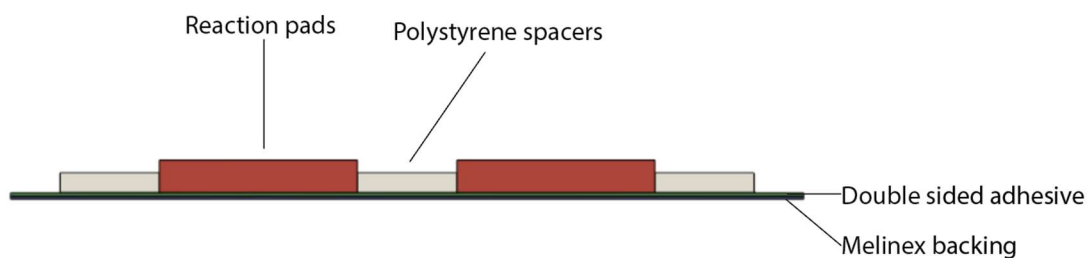


Figure 2: Schematic layout of the paper device.

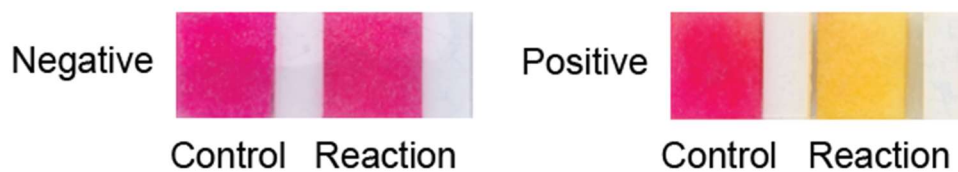


Figure 3: Typical colorimetric results of a negative and positive run. Controls are RT-LAMP reactions without LAMP primers included and positive reactions have 800 copies/ μ L spiked into 5% saliva.

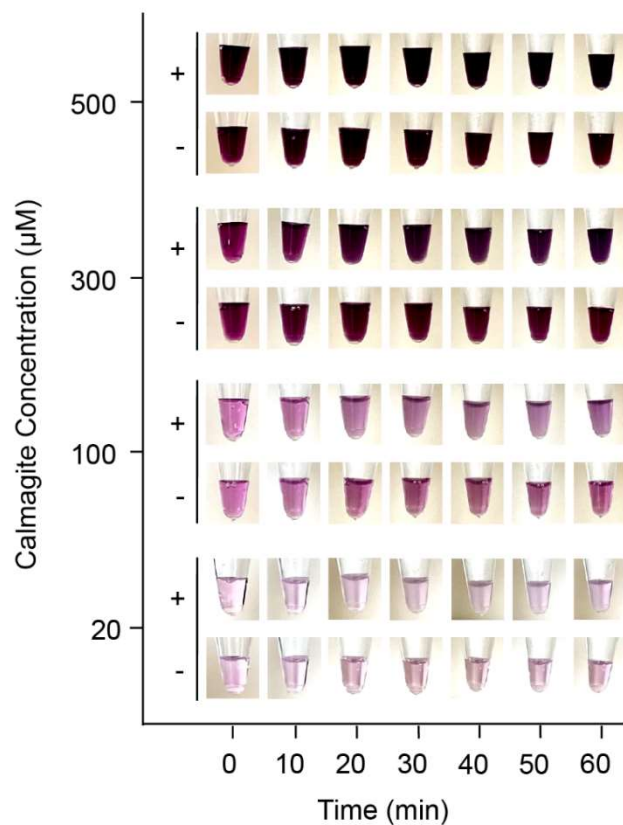


Figure 4: LAMP detection with increasing concentrations of calmagite (magnesium indicator). The lolB.3 primer set targeting *Histophilus somni* (HS) genomic DNA was used. Positive reactions were spiked with 5 µL of HS gDNA at a concentration of 0.2 ng/µL. Negative reactions used 5 µL of nuclease-free water. The total reaction volume is 25 µL. Data was collected by Ana Pascual-Garrigos.

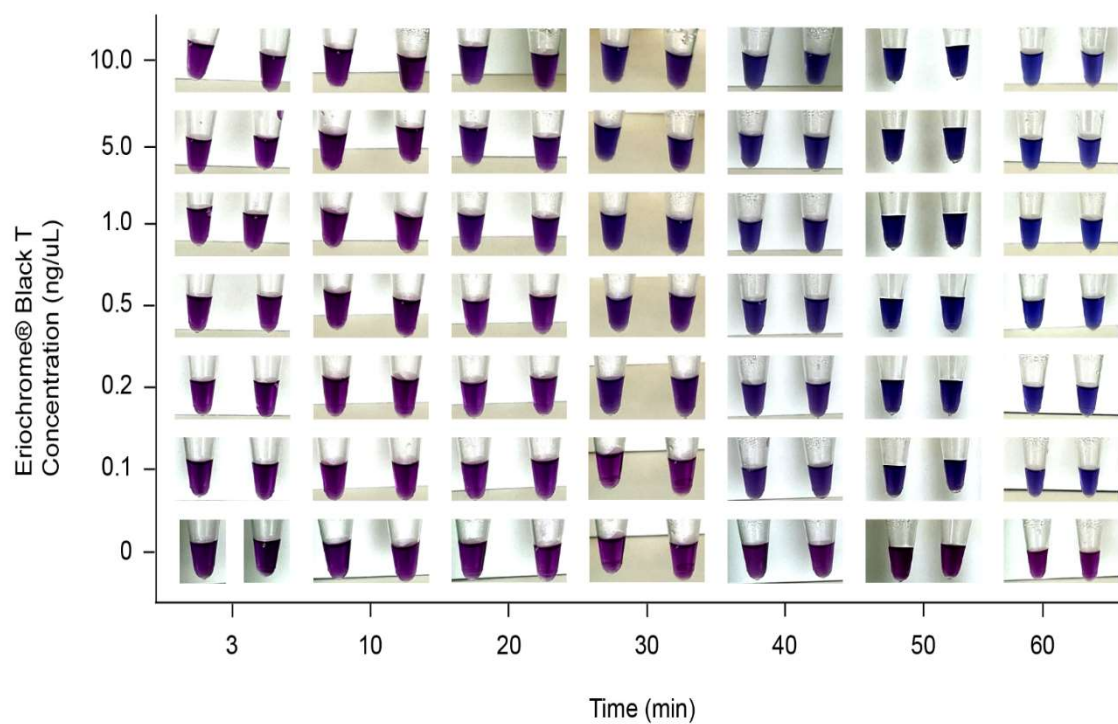


Figure 5: LAMP detection with increasing concentrations of Eriochrome® Black T (magnesium indicator). Primer sets and reaction conditions were the same as those in Figure S1. Data was collected by Ana Pascual-Garrigos.

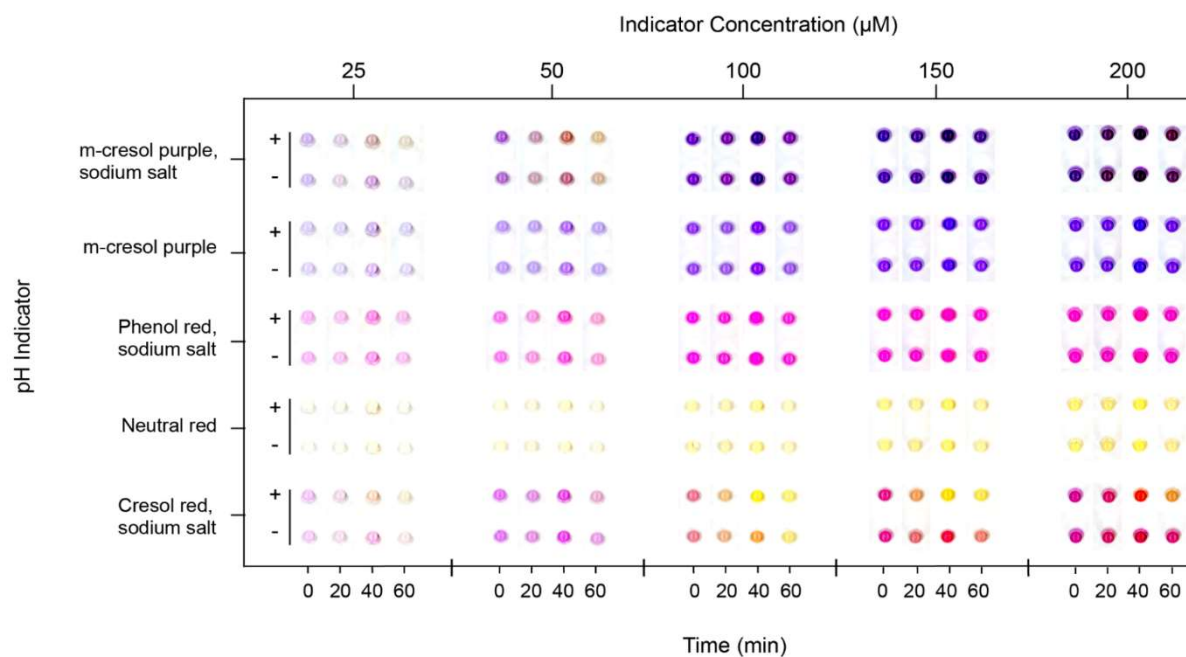


Figure 6: RT-LAMP detection with increasing concentrations of cresol red sodium salt, Neutral red, Phenol red sodium salt, m-cresol purple, and m-cresol purple sodium salt in solution (pH indicator). The N.10 primer set targeting the N gene of SARS-CoV-2 was used. Positive reactions were spiked with 5 μ L of in-vitro transcribed N gene RNA at a concentration of 10.2 ng/ μ L. Negative reactions used μ L of nuclease-free water. Data was collected by Ana Pascual-Garrigos.

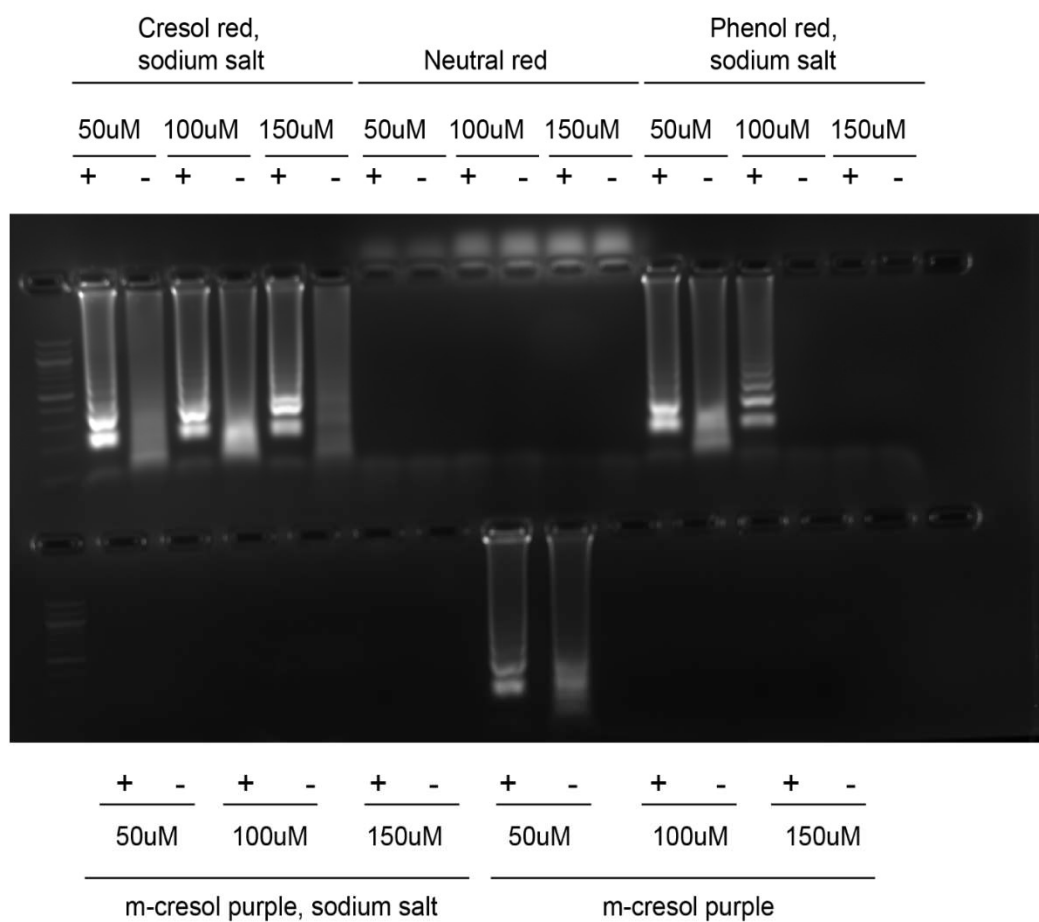


Figure 7: Endpoint gel electrophoresis scans of the RT-LAMP products (60 mins) in Figure 6. Data was collected by Ana Pascual-Garrigos.

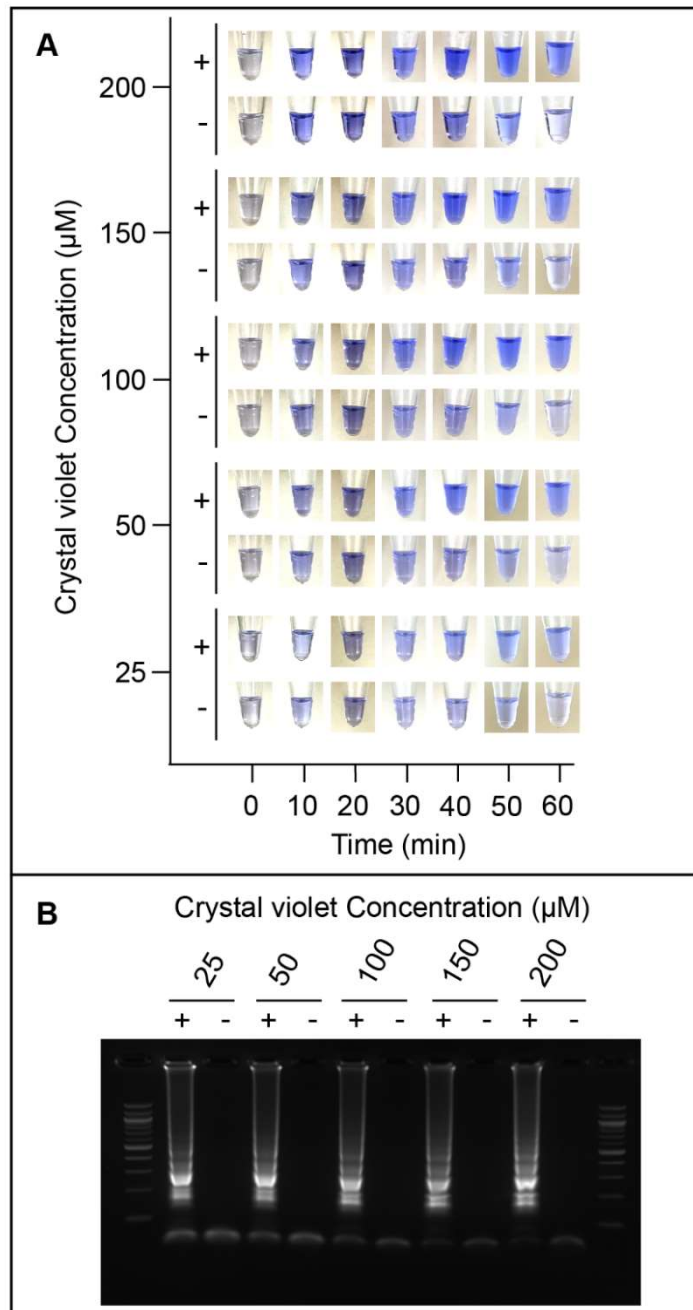


Figure 8: LAMP detection with intercalating dye, Crystal violet a) in solution and b) associated in gel electrophoresis (2% agarose) scan of the products at 60 minutes. Data was collected by Ana Pascual-Garrigos.

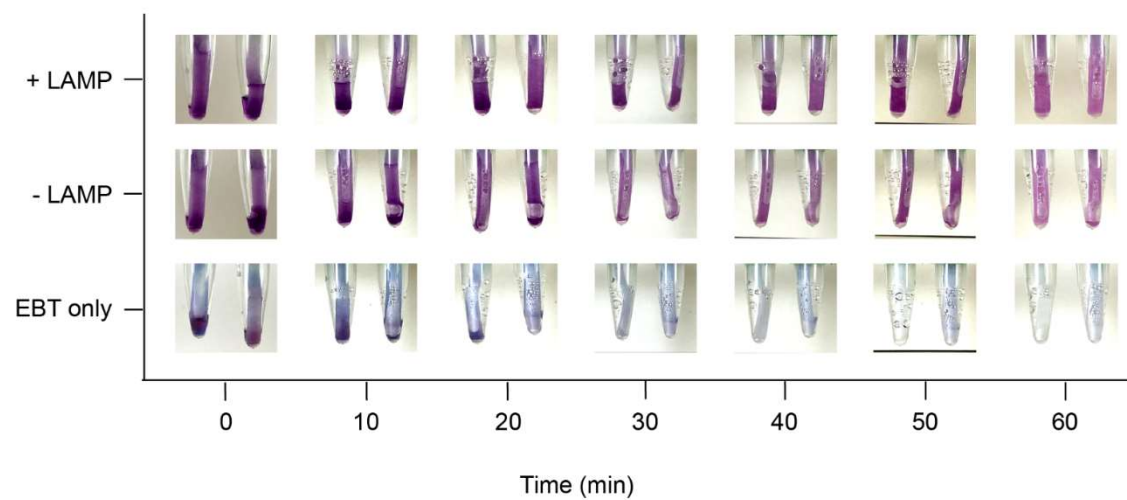


Figure 9: LAMP detection with increasing concentrations of Eriochrome® Black T on chromatography paper in PCR tubes (magnesium indicator). Data was collected by Ana

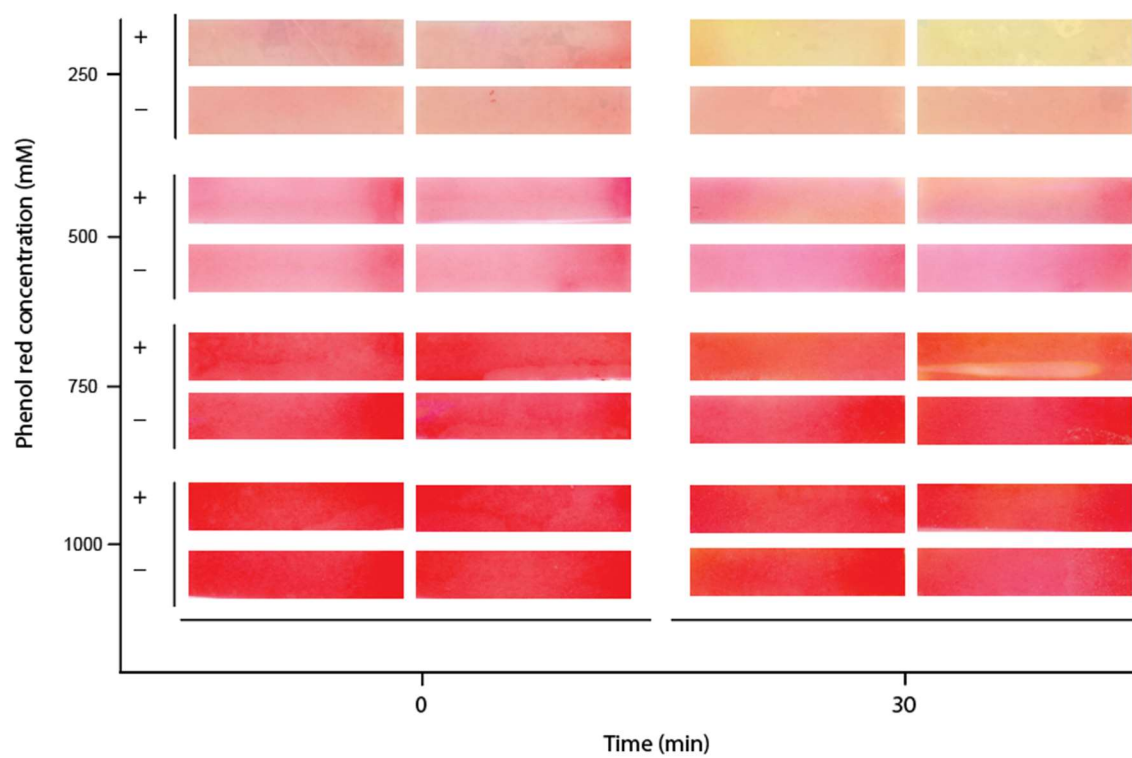


Figure 10: LAMP detection with increasing concentrations of Phenol red on Grade 1 chromatography paper.

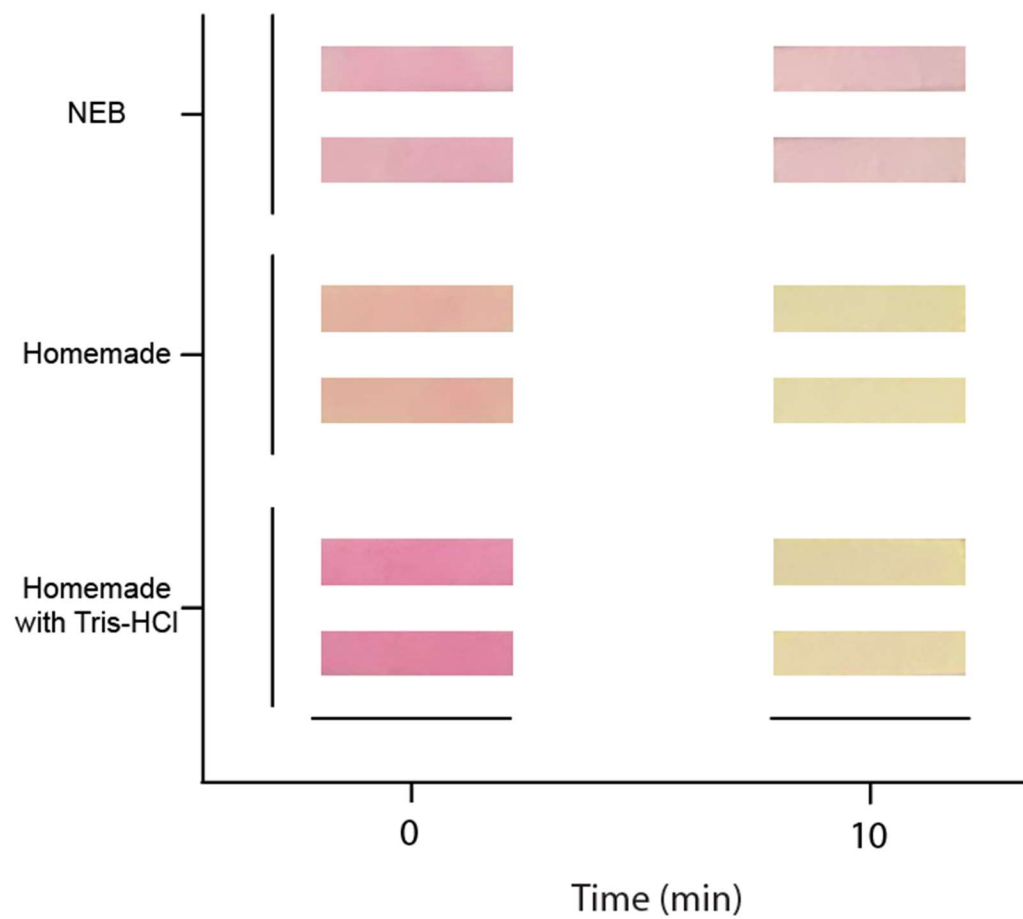


Figure 11: Different LAMP formulations drying on Grade 1 chromatography paper. All formulations were adjusted to pH 8.0. Tris-HCl concentration is 20mM.

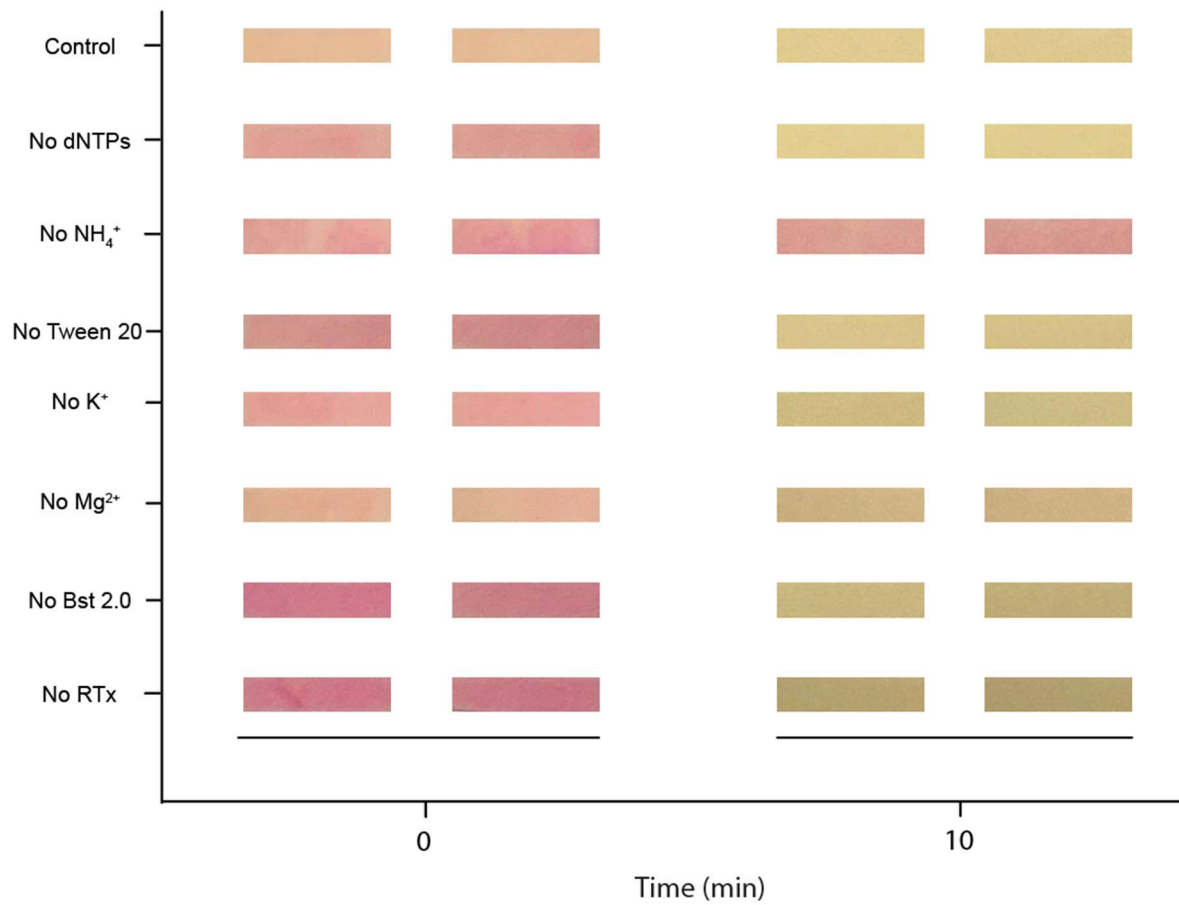


Figure 12: Different LAMP formulations eliminating one component at a time and drying on Grade 1 chromatography paper. All LAMP formulations were adjusted to pH 8.0 according to a pH probe. A color difference between conditions at 0 min is due to the fast acidification process once the reagent is applied to the paper.

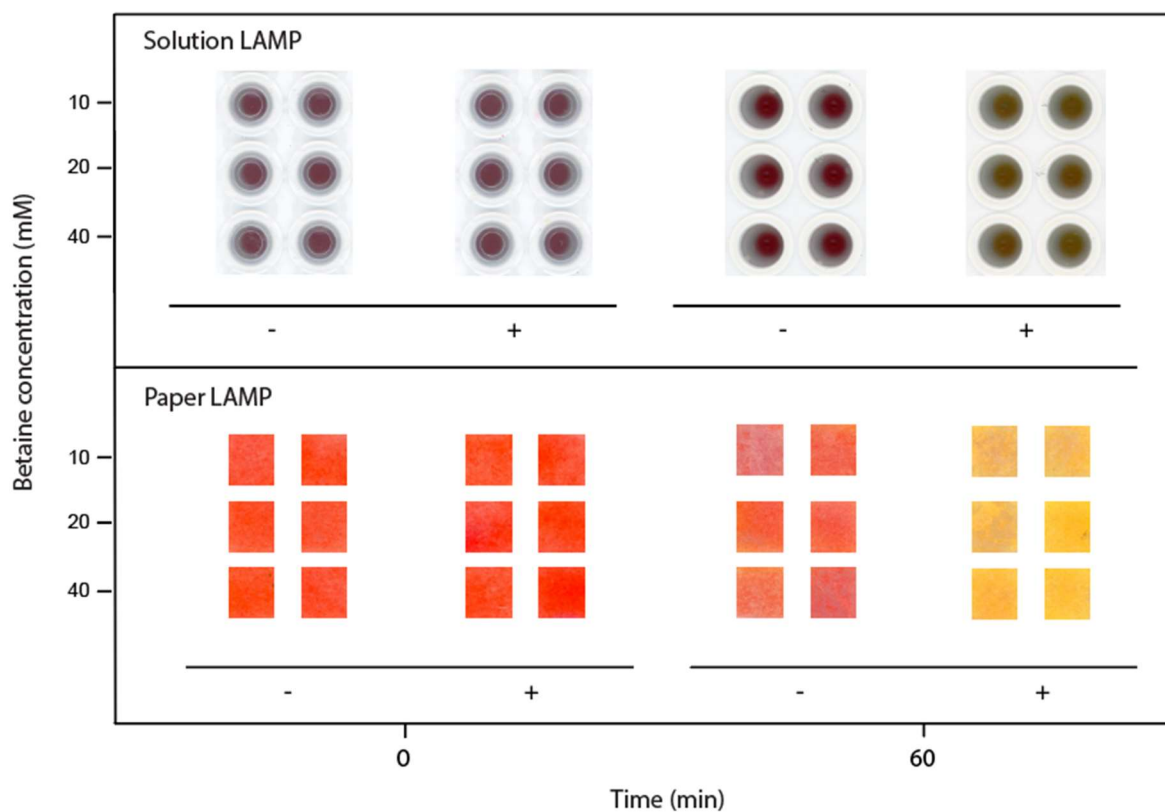


Figure 13: LAMP formulation using different betaine concentrations substituting ammonium ions as the destabilizing agent. Reactions were performed in solution and Grade 22 chromatography paper simultaneously.

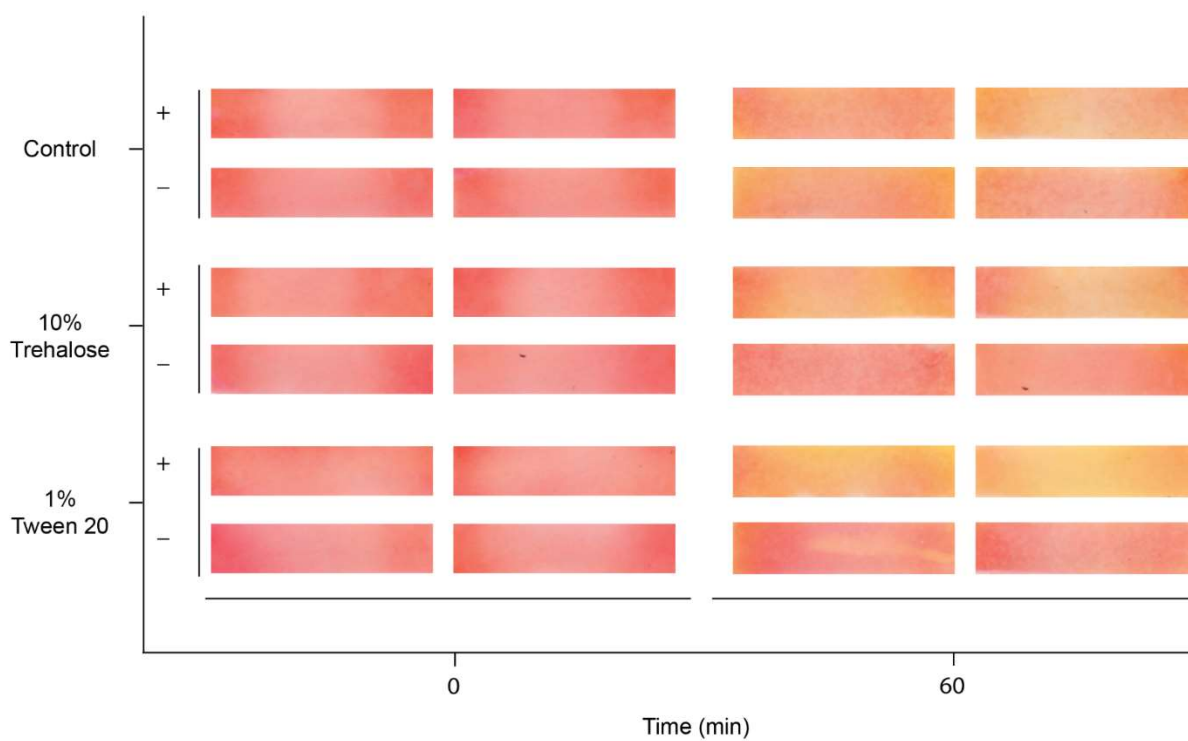


Figure 14: Colorimetric RT-LAMP results with the inclusion of Trehalose or Tween 20 at the given concentration. The orf7ab.I primer set was used and heat-inactivated SARS-CoV-2 at a concentration of 1×10^5 copies per reaction was spiked into 5% saliva.

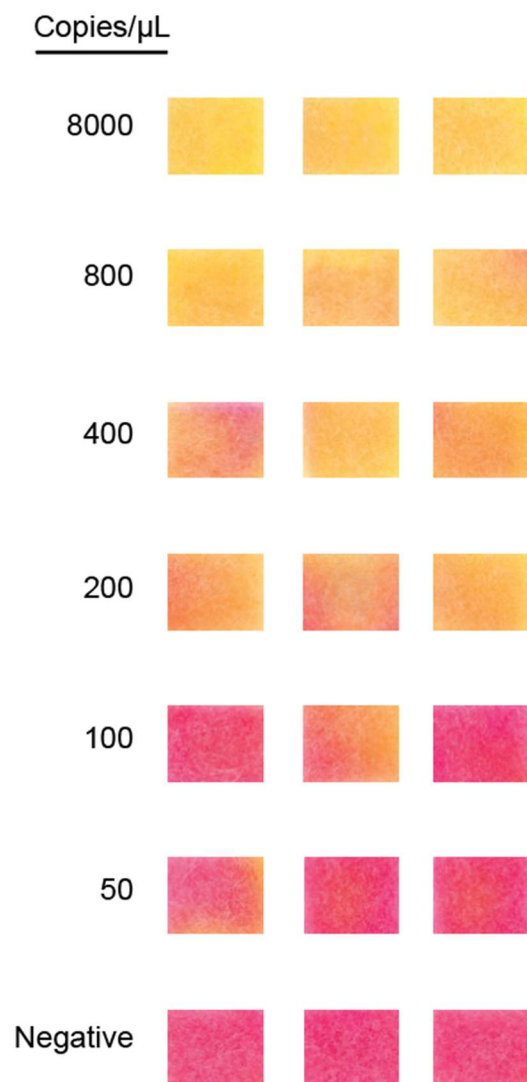


Figure 15: Colorimetric LoD on paper using Heat-inactivated virus at the indicated concentration in 5% saliva. The LoD of the assay was determined as 200 copies of virus per μ L of whole saliva.

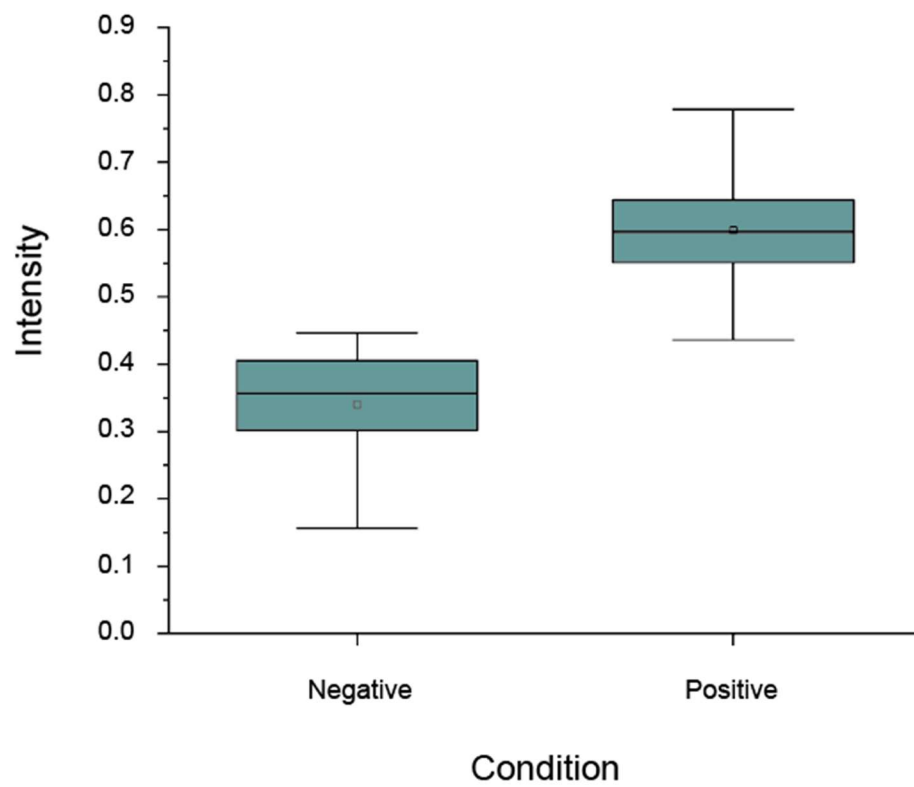


Figure 16: Box plot for the green channel intensity of 30 positive and 30 negative results of RT-LAMP on paper.

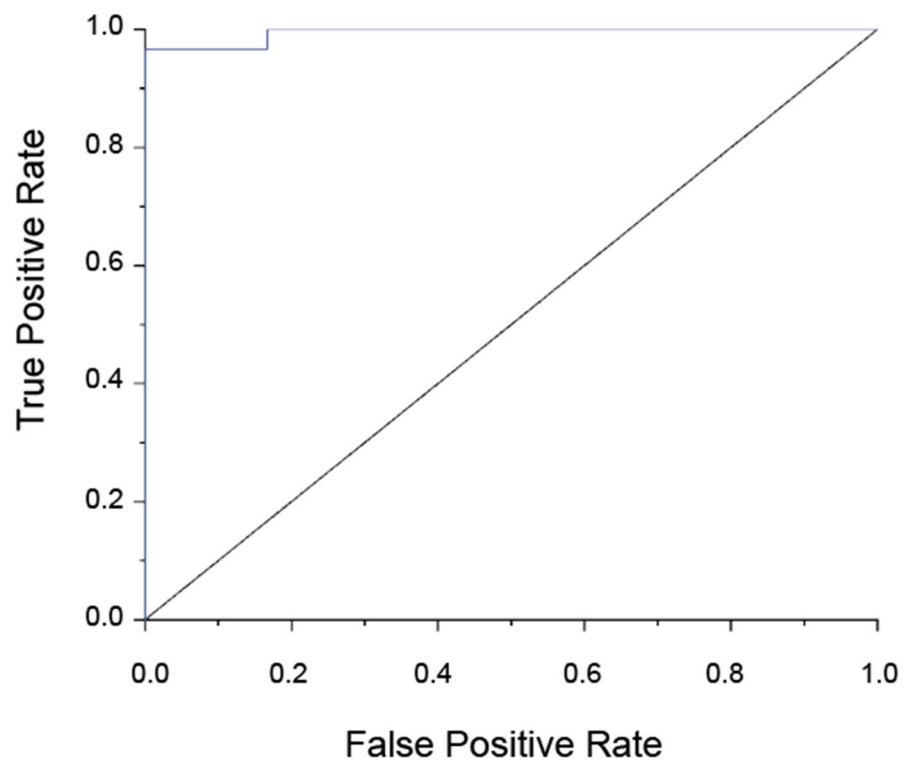


Figure 17: Receiver-operator (ROC) curve for 30 positive and 30 negative results of RT-LAMP on paper.

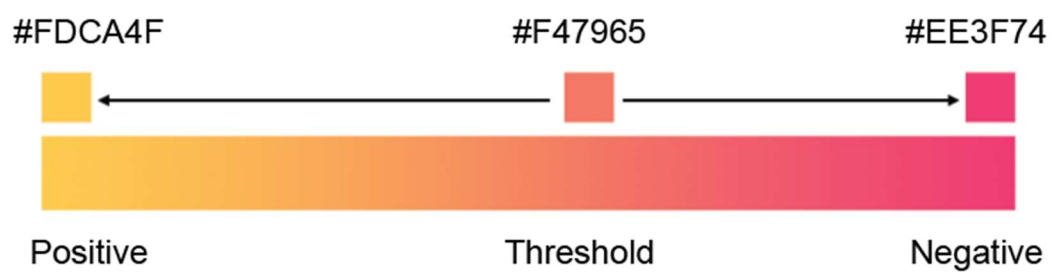


Figure 18: Color gradient of possible results derived from the colorimetric results of

5. CONCLUSIONS

This paper-based LAMP platform has the following advantages: i) it does not require RNA extraction, ii) it requires minimal operator training, iii) it can be fabricated using roll-to-roll methods to achieve millions of tests, iv) it provides a colorimetric response visible to the naked eye, v) it is amenable to point-of-care use, and vi) it provides results in less than 60 minutes.

Three limitations of the current approach are i) the LoD of this assay is higher than a conventional qPCR test. ii) although the red-yellow color transition is vivid, variations in perception of color could affect the interpretation of results, especially with lower virus concentrations. This could be overcome by color quantification software, for example using a cellphone to capture the image and quantify color.

Due to the simplicity and scalability of this test, I envision that it could be used widely. Since the test is based on nucleic acids, it can be rapidly adapted for future outbreaks as well by designing and screening new primer sets.

REFERENCES

- Ai, T., Yang, Z., Hou, H., Zhan, C., Chen, C., Lv, W., Tao, Q., Sun, Z., & Xia, L. (2020). Correlation of Chest CT and RT-PCR Testing for Coronavirus Disease 2019 (COVID-19) in China: A Report of 1014 Cases. *Radiology*, 296(2), E32–E40. <https://doi.org/10.1148/radiol.2020200642>
- Arnaout, R., Lee, R. A., Lee, G. R., Callahan, C., Yen, C. F., Smith, K. P., Arora, R., & Kirby, J. E. (2020). SARS-CoV2 Testing: The Limit of Detection Matters. *BioRxiv*, 2020.06.02.131144. <https://doi.org/10.1101/2020.06.02.131144>
- Baliga, S., Muglikar, S., & Kale, R. (2013). Salivary pH: A diagnostic biomarker. *Journal of Indian Society of Periodontology*, 17(4), 461–465. <https://doi.org/10.4103/0972-124X.118317>
- Chen, L., Liu, W., Zhang, Q., Xu, K., Ye, G., Wu, W., Sun, Z., Liu, F., Wu, K., Zhong, B., Mei, Y., Zhang, W., Chen, Y., Li, Y., Shi, M., Lan, K., & Liu, Y. (2020). RNA based mNGS approach identifies a novel human coronavirus from two individual pneumonia cases in 2019 Wuhan outbreak. *Emerging Microbes & Infections*, 9(1), 313–319. <https://doi.org/10.1080/22221751.2020.1725399>
- Fernandes, N. (2020). *Economic Effects of Coronavirus Outbreak (COVID-19) on the World Economy* (SSRN Scholarly Paper ID 3557504). Social Science Research Network. <https://doi.org/10.2139/ssrn.3557504>
- Francois, P., Tangomo, M., Hibbs, J., Bonetti, E.-J., Boehme, C. C., Notomi, T., Perkins, M. D., & Schrenzel, J. (2011). Robustness of a loop-mediated isothermal amplification reaction for diagnostic applications. *FEMS Immunology and Medical Microbiology*, 62(1), 41–48. <https://doi.org/10.1111/j.1574-695X.2011.00785.x>
- Hayashida, K., Kajino, K., Hachaambwa, L., Namangala, B., & Sugimoto, C. (2015). Direct Blood Dry LAMP: A Rapid, Stable, and Easy Diagnostic Tool for Human African Trypanosomiasis. *PLOS Neglected Tropical Diseases*, 9(3), e0003578. <https://doi.org/10.1371/journal.pntd.0003578>

- Hsieh, K., Mage, P. L., Csordas, A. T., Eisenstein, M., & Soh, H. T. (2014). Simultaneous elimination of carryover contamination and detection of DNA with uracil-DNA-glycosylase-supplemented loop-mediated isothermal amplification (UDG-LAMP). *Chemical Communications*, 50(28), 3747–3749. <https://doi.org/10.1039/C4CC00540F>
- Huang, Y., Yang, C., Xu, X., Xu, W., & Liu, S. (2020). Structural and functional properties of SARS-CoV-2 spike protein: Potential antiviral drug development for COVID-19. *Acta Pharmacologica Sinica*, 41(9), 1141–1149. <https://doi.org/10.1038/s41401-020-0485-4>
- Kaneko, H., Kawana, T., Fukushima, E., & Suzutani, T. (2007). Tolerance of loop-mediated isothermal amplification to a culture medium and biological substances. *Journal of Biochemical and Biophysical Methods*, 70(3), 499–501. <https://doi.org/10.1016/j.jbbm.2006.08.008>
- Kucirka, L. M., Lauer, S. A., Laeyendecker, O., Boon, D., & Lessler, J. (2020). Variation in False-Negative Rate of Reverse Transcriptase Polymerase Chain Reaction–Based SARS-CoV-2 Tests by Time Since Exposure. *Annals of Internal Medicine*. <https://doi.org/10.7326/M20-1495>
- Kumar, S., Gallagher, R., Bishop, J., Kline, E., Buser, J., Lafleur, L., Shah, K., Lutz, B., & Yager, P. (2020). Long-term dry storage of enzyme-based reagents for isothermal nucleic acid amplification in a porous matrix for use in point-of-care diagnostic devices. *Analyst*, 145(21), 6875–6886. <https://doi.org/10.1039/D0AN01098G>
- Lalli, M. A., Langmade, S. J., Chen, X., Fronick, C. C., Sawyer, C. S., Burcea, L. C., Wilkinson, M. N., Fulton, R. S., Heinz, M., Buchser, W. J., Head, R. D., Mitra, R. D., & Milbrandt, J. (2020). Rapid and extraction-free detection of SARS-CoV-2 from saliva with colorimetric LAMP. *MedRxiv*. <https://doi.org/10.1101/2020.05.07.20093542>
- Mallepaddi, P. C., Lai, M.-Y., Podha, S., Ooi, C.-H., Liew, J. W.-K., Polavarapu, R., & Lau, Y.-L. (2018). Development of Loop-Mediated Isothermal Amplification–Based Lateral Flow Device Method for the Detection of Malaria. *The American Journal of Tropical Medicine and Hygiene*, 99(3), 704–708. <https://doi.org/10.4269/ajtmh.18-0177>
- Mohapatra, R. K., Pintilie, L., Kandi, V., Sarangi, A. K., Das, D., Sahu, R., & Perekhoda, L. (2020). The recent challenges of highly contagious COVID-19, causing respiratory infections: Symptoms, diagnosis, transmission, possible vaccines, animal models, and immunotherapy. *Chemical Biology & Drug Design*. <https://doi.org/10.1111/cbdd.13761>

- PCR Setup—Six Critical Components to Consider—US.* (n.d.). Retrieved February 16, 2021, from [//www.thermofisher.com/us/en/home/life-science/cloning/cloning-learning-center/invitrogen-school-of-molecular-biology/pcr-education/pcr-reagents-enzymes/pcr-component-considerations.html](http://www.thermofisher.com/us/en/home/life-science/cloning/cloning-learning-center/invitrogen-school-of-molecular-biology/pcr-education/pcr-reagents-enzymes/pcr-component-considerations.html)
- Schrader, C., Schielke, A., Ellerbroek, L., & Johne, R. (2012). PCR inhibitors – occurrence, properties and removal. *Journal of Applied Microbiology*, 113(5), 1014–1026. <https://doi.org/10.1111/j.1365-2672.2012.05384.x>
- Seok, Y., Joung, H.-A., Byun, J.-Y., Jeon, H.-S., Shin, S. J., Kim, S., Shin, Y.-B., Han, H. S., & Kim, M.-G. (2017). A Paper-Based Device for Performing Loop-Mediated Isothermal Amplification with Real-Time Simultaneous Detection of Multiple DNA Targets. *Theranostics*, 7(8), 2220–2230. <https://doi.org/10.7150/thno.18675>
- Tang, Y.-W., Schmitz, J. E., Persing, D. H., & Stratton, C. W. (2020). Laboratory Diagnosis of COVID-19: Current Issues and Challenges. *Journal of Clinical Microbiology*, 58(6), e00512-20, /jcm/58/6/JCM.00512-20.atom. <https://doi.org/10.1128/JCM.00512-20>
- Yetisen, A. K., Akram, M. S., & Lowe, C. R. (2013). Paper-based microfluidic point-of-care diagnostic devices. *Lab on a Chip*, 13(12), 2210–2251. <https://doi.org/10.1039/c3lc50169h>
- Zhang, Y., Ren, G., Buss, J., Barry, A. J., Patton, G. C., & Tanner, N. A. (2020). Enhancing Colorimetric LAMP Amplification Speed and Sensitivity with Guanidine Chloride. *BioRxiv*, 2020.06.03.132894. <https://doi.org/10.1101/2020.06.03.132894>
- Zhu, J., Guo, J., Xu, Y., & Chen, X. (2020). Viral dynamics of SARS-CoV-2 in saliva from infected patients. *The Journal of Infection*, 81(3), e48–e50. <https://doi.org/10.1016/j.jinf.2020.06.059>